British Journal of Cancer www.nature.com/bjc

ARTICLE

Translational Therapeutics

Targeted therapy for drug-tolerant persister cells after imatinib treatment for gastrointestinal stromal tumours

Tomo Ishida[1], Tsuyoshi Takahashi[1✉], Yukinori Kurokawa[1], Toshirou Nishida[2], Seiichi Hirota[3], Satoshi Serada[4], Minoru Fujimoto[4], Tetsuji Naka[4], Ryugo Teranishi[1], Takuro Saito[1], Kotaro Yamashita[1], Koji Tanaka[1], Kazuyoshi Yamamoto[1], Tomoki Makino[1], Makoto Yamasaki[1], Kiyokazu Nakajima[1], Hidetoshi Eguchi[1] and Yuichiro Doki[1]

BACKGROUND: Despite the effectiveness of tyrosine kinase inhibitors (TKI), gastrointestinal stromal tumours (GIST) develop after the withdrawal of TKI. Based on previous studies, a subpopulation of drug-tolerant cells called "persister cells" may be responsible for the recurrence and have thus, gained attention as a novel target in cancer therapy.
METHODS: The metabolic changes were investigated in imatinib-derived persister GIST cells. We investigated the efficacy and the mechanism of GPX4 inhibitor, which is known as a major inducer of "ferroptosis". We also evaluated the effects of RSL3 to the gefitinib-derived persister lung cancer cells.
RESULTS: We demonstrated a downregulation of glucose metabolism, subsequent decrease in the glutathione level and sensitivity to glutathione peroxidase 4 (GPX4) inhibitor, RSL3 in persister cells. As the cell death induced by RSL3 was found to be "iron-dependent" and "caspase-independent", loss of GPX4 function could have possibly induced selective persister cell ferroptotic death. In the xenograft model, we confirmed the inhibition of tumour regrowth after discontinuation of imatinib treatment. Moreover, RSL3 prevented the growth of gefitinib-derived persister lung cancer cells.
CONCLUSIONS: RSL3 combined with TKI may be a promising therapy for both GIST and epidermal growth factor receptor-mutated lung cancer.

British Journal of Cancer (2021) 125:1511–1522; https://doi.org/10.1038/s41416-021-01566-9

BACKGROUND

Gastrointestinal stromal tumour (GIST) is a mesenchymal tumour of the gastrointestinal tract in which gain-of-function mutations in the *KIT* or *PDGFRA* receptor tyrosine kinase are crucial for initiating oncogenic events [1, 2]. Therefore, in most of the patients with primary GIST, the inhibition of KIT or PDGFRA signaling with tyrosine kinase inhibitors (TKI) successfully impairs tumour growth [3, 4]. Among all TKI, imatinib mesylate (Gleevec, Novartis Oncology, Basel, Switzerland) substantially improved progression-free and overall survival in patients with advanced GIST [5]. However, in clinical practice, imatinib treatment for GIST has been associated with some problems, including tumour recurrence or regrowth after the withdrawal of imatinib therapy and the development of drug resistance [6–8]. The BFR14 trial, which investigated the effect of prolonged imatinib treatment in patients with advanced GIST, revealed that interruption of imatinib therapy resulted in rapid disease progression in most patients with advanced GIST and that imatinib treatment should be maintained indefinitely even in patients with complete response [9]. This finding strongly suggests that most patients have widespread, disseminated, residual viable disease after imatinib treatment. Furthermore, the survival of these drug-tolerant "persister cells" may play a key role in tumour relapse and subsequent drug resistance. In addition, the involvement of persister cells has been reported in other molecular-targeted therapies, including gefitinib treatment in epidermal growth factor receptor (EGFR)-mutant lung cancer [9], and has garnered attention as an important issue in molecular-targeted therapy. Thus, targeting of persister cells may present a therapeutic opportunity to impede tumour relapse and prevent drug resistance.

Ferroptosis is a new type of cell death that is characterised by overwhelming iron-dependent lipid peroxidation [10, 11], which facilitates the selective elimination of some tumour cells or can be activated in specific pathological states, such as ischemia/reperfusion injury or neurodegeneration [12]. The development of ferroptosis is dependent upon intracellular free iron (Fe^{2+}), and is morphologically, biochemically and genetically distinct from apoptosis, necrosis and other types of cell death [13]. Glutathione (GSH) is one of the antioxidants that plays a key role in protecting cells against oxidative stress, including ferroptosis [11, 14]. In a previous study, a decrease in GSH levels in persister cells and vulnerability to glutathione peroxidase 4 (GPX4) inhibitors, which are known to be major inducers of ferroptosis, has been reported [15].

[1]Department of Gastroenterological Surgery, Graduate School of Medicine, Osaka University, 2-2-E2, Yamadaoka, Suita, Osaka 565-0871, Japan. [2]Department of Surgery, Japan Community Health Care Organization Osaka Hospital, 4-2-78, Fukushima, Fukushima-ku, Osaka, Japan. [3]Department of Surgical Pathology, Hyogo College of Medicine, 1-1, Mukogawacho, Nishinomiya, Hyogo, Japan. [4]Center for Intractable Disease, Kochi University, Nankoku, Japan. ✉email: ttakahashi2@gesurg.med.osaka-u.ac.jp

Received: 28 December 2020 Revised: 24 August 2021 Accepted: 21 September 2021
Published online: 5 October 2021

In this study, we aimed to clarify the nature of persister cells and to verify the validity of GPX4 inhibitor in targeted therapy for persister cells.

METHODS

Cell preparation and chemical reagents

We used the established human GIST cell line, GIST-T1 (Cosmobio, Tokyo, Japan) in this study. This *KIT* exon 11-mutant cell line is characterised by a heterozygous deletion of 57 bases, which makes it sensitive to imatinib [16]. GIST-T1 cells were cultured in Dulbecco's modified Eagle's medium supplemented with 10% foetal bovine serum (FBS) (GE Healthcare, Little Chalfont, Buckinghamshire, UK) and 100 U/mL penicillin and 100 µg/mL streptomycin (Invitrogen, Carlsbad, CA) at 37 °C in a humid atmosphere containing 5% CO_2. To generate imatinib-resistant cell lines, GIST-T1 cells were cultured with increasing concentrations of imatinib, and the imatinib-resistant cell lines, R2, R8 and R9 [17] were established and maintained under a constant concentration of 1 µM imatinib. For 9 days in glucose-free medium, the volume of FBS was increased to 50%. Cells from the human non-small cell lung cancer cell line PC9 were cultured in Roswell Park Memorial Institute (RPMI) medium with FBS and penicillin/streptomycin. Cells and mice were treated with imatinib mesylate (Tocris, Bristol, UK), RSL3, a GPX4 inhibitor (Selleck chemicals, Houston, TX), 5-fluorouracil (5-FU; Wako Pure Industries, Osaka, Japan), deferoxamine mesylate, iron-chelator (Sigma–Aldrich, St. Louis, MO), Ferrostatin-1, anti-ferroptosis reagent (Sigma–Aldrich) and Z-VAD, pan-caspase inhibitor (Promega, Madison, WI).

Metabolome analysis

Metabolome analysis was performed at Human Metabolome Technologies (HMT, Tsuruoka, Japan, http://humanmetabolome.com). Cellular metabolites from GIST-T1 cells and GIST-T1 cells treated with 20 nM imatinib for 3 and 14 days, respectively, were generated according to the manufacturer's protocol. Metabolome analysis was performed by capillary electrophoresis time-of-flight mass spectrometry (CE-TOFMS). Metabolite peaks were quantified and normalised according to protein concentrations.

Persister cell derivation and RSL3 treatments

Persister cells were derived through the treatment of GIST-T1 cells with 2 µM imatinib and of EGFR-mutant non-small cell lung cancer PC9 with 2 µM gefitinib or with 10 µM 5-FU for at least 9 days, with fresh drug added every 3 days. Unless otherwise noted, RSL3 were added to pre-derived persister cells plated in 96-well tissue culture plates that were maintained under constant drug exposure throughout the subsequent RSL3 treatment. Cell viability was assessed using CellTiter-Glo (Promega) after 72 h of RSL3 treatment. Pre-derived GIST-T1 persister cells from the 2 µM imatinib line were allowed to regrow upon removal of imatinib for 7 days and were then examined in a cell viability assay and a cell proliferation assay.

Flow cytometric analysis

Flow cytometry was performed with the BD FACS Canto II (BD Biosciences, Franklin Lakes, NJ). Doublet cells were eliminated with FSC-A/FSC-H and SSC-A/SSC-H. Propidium iodide (PI; Dojindo Molecular Technologies, Kumamoto, Japan), RNase (Wako), CellROX Deep Red (Thermo Fisher Scientific, Waltham, MA), APC-Annexin V (BioLegend, San Diego, CA) and PI (BioVision, San Fransisco, CA) were used for cell labeling.

Chemosensitivity assay

Cells were plated in 96-well white plates at a density of 2×10^3 cells per well and incubated for 24 h. Cell viability was evaluated with CellTiter-Glo Assay (Promega) and was visualised using a microplate luminometer (Centro LB960, Berthold Technologies, Bad Wildbad, Germany). The viability rate was expressed as the percentage of absorbance for cells at each concentration versus that of the control. Experiments were performed with six replicate wells for each sample, and the data are presented as mean ± standard deviation (SD).

Cell proliferation assay

Cells were plated in 96-well plates at a density of 10^3 cells per well and incubated for 12 h (baseline). Cell proliferation was evaluated with Cell Counting Kit-8 (Dojindo Molecular Technologies, Inc) at the indicated time points. The absorption (optical density [OD]) was measured at a wavelength of 450 nm, with a reference wavelength of 630 nm, by using a microplate reader (Model 680; Bio-Rad Laboratories, Hercules, CA). The growth rate was expressed as the percentage of absorbance for cells at each timepoint versus that of the baseline. Experiments were performed with six replicate wells for each sample, and the data are presented as mean ± SD.

Cell-cycle assay

For cell-cycle analysis by PI staining, cells were fixed in cold 70% ethanol for 2 h at 4 °C. After spinning at $900 \times g$ in a centrifuge and carefully discarding the supernatant, 50 µL RNase (from a 100 µg/mL stock solution) and 200 µL PI (from a 50 µg/mL stock solution) were added to the pellet, followed by incubation for 15 min at 37 °C. A FACS Canto II instrument (BD Biosciences, San Jose, CA, USA) was used for analysis and cell sorting.

Sphere-formation assay

Single cells were plated in 96-well ultra-low attachment plates (Corning Inc., Corning, NY) at a density of 1000 cells per well and grown in Dulbecco's modified Eagle's medium/F-12 serum-free medium (Invitrogen) that was supplemented with 20 ng/mL epithelial growth factor, 10 ng/mL basic fibroblast growth factor-2 (Pepro Tech, Cranbury, NJ) and 100 µg/mL penicillin G at 37 °C in a humidified atmosphere of 95% air and 5% CO_2. We counted the number of spheres at ≥100 µm in all wells and evaluated differences in the average number per well at 3 weeks after seeding.

GSH, GSH reductase, NADPH and glucose-uptake measurements

GSH-Glo and Glucose Uptake-Glo Assay Kits (Promega) were used to measure GSH levels in 2000 cells and glucose-uptake levels in 5000 cells per replicate according to the manufacturer's instructions. GSH-Glo Assay and Glucose Uptake-Glo Assay were read using a microplate luminometer (Centro LB960, Berthold Technologies).

The NADP/NADPH Assay Kit WST (Dojindo Molecular Technologies, Inc, Japan) was used to measure NADPH levels in 5000 cells per replicate according to the manufacturer's instructions. Similarly, the OxiSelect Glutathione Reductase Assay Kit (Cell Biolabs. Inc., San Diego, CA) was used to measure GSH reductase levels in 1,000,000 cells per replicate, according to the manufacturer's instructions. The NADP/NADPH and GSH reductase assays were measured at a wavelength of 450 and 405 nm, respectively, using a microplate reader (Model 680; Bio-Rad Laboratories). OxiSelect Total Glutathione Assay Kit was used to measure GSH levels in clinical samples according to the manufacturer's instructions.

Caspase activity measurements

Caspase 3/7-Glo Assay Kits (Promega) were used to measure caspase activity in 2000 cells per replicate according to the manufacturer's instructions. Caspase 3/7-Glo Assay were read using a microplate luminometer (Centro LB960, Berthold Technologies).

Western blotting analysis

Whole-cell lysates were prepared as described previously [18], and protein concentrations were determined using the Bio-Rad protein assay (Bio-Rad Laboratories, CA). Electrophoresis, immunoblotting and chemiluminescence detection were undertaken as described previously. Primary antibodies to GPX4 (ab125066) and hypoxia-inducible factor (HIF)-1α (ab51608) were procured from Abcam (Cambridge, MA, USA), and the secondary antibody (horse-radish peroxidase-conjugated goat anti-rabbit IgG) was obtained from Cell Signaling Technology (Danvers, MA).

GIST cell xenograft mouse models (subcutaneous tumour models)

Since it is essential to provide the efficacy and safety of the drug, RSL3 in an animal model, we carried out animal experiments in this study. This study received IRB approval from Osaka University Hospital (protocol number 25–062–011). All animal experiments were conducted according to the institutional ethical guidelines of Osaka University for animal experimentation. Mice were housed in a temperature-controlled room with 12 h light/12 h dark cycle and provided free access to water and diets in the laboratory of Graduate School of Medicine, Osaka University. For the xenograft experiments, the mice were anaesthetised by 3% isoflurane. We established a mouse xenograft model by inoculating the

mice subcutaneously with GIST cells. For cell inoculation, 5.0×10^6 GIST-T1 cells in 200 µL 1:1 (v/v) Dulbecco's modified Eagle's medium/Matrigel (Becton Dickinson, Franklin Lakes, NJ) were injected subcutaneously into the dorsolateral aspect of male nude mice (6 weeks old; CLEA Japan, Inc., Meguro-ku, Japan). Mice were observed daily for tumour growth. We evaluated the therapeutic effects of combining imatinib with a RSL3 in vivo. When the diameter of either side of the subcutaneous tumours reached 300 mm^3, tumour-bearing animals were open-label randomly assigned to one of four groups using the sequentially numbered container method. And mice, whose tumours did not reached 300 mm^2 in 40 days, were excluded. We administered control (phosphate buffer saline plus vehicle), RSL3 or imatinib alone, or a combination (imatinib plus RSL3). The vehicle solution and RSL3 contained 5% dimethyl sulfoxide (DMSO) (Wako, Japan) and 2% Tween 80 (Sigma–Aldrich US). Imatinib was dosed intraperitoneally at 100 mg/kg once every day for 9 days. RSL3 in 5% DMSO and 2% Tween 80 was administered intraperitoneally on day 9 at 50 mg/kg/day. A total of four animals, one from each group, were placed in the same cage. To evaluate changes in tumour volume after each therapeutic regimen, we continued to measure tumour volume once every 3 days until 21 days from the initiation of therapy. Tumour volumes were determined by measuring the tumour length and width: volume = (width^2 × length)/2. All control mice received an equal volume of DMSO. Mice were anaesthetised by 3% isoflurane and euthanised via cervical dislocation 21 days after the first treatment. Subsequently, the tumours were resected.

Immunohistochemistry

Subcutaneously implanted tumours were harvested and embedded in paraffin for immunohistochemical analysis. After antigen retrieval, treatment and blockade of endogenous peroxidase activity, the 4 µm-thick sections were stained with rabbit anti-human c-kit antibodies (1:200 dilution; Cell Signaling Technology, Danvers, MA), rabbit anti-human Ki-67 antibodies (1:200 dilution: Abcam, Cambridge, MA) and rabbit anti-human GPX4 antibodies (1:100 dilution; Abcam).

Clinical GIST specimens

Clinical GIST samples were obtained from Osaka University, Japan, after obtaining informed consent from the patients and approval from the Research Ethics Board of Osaka University (approval no. 08226-14).

Microarray experiments

Microarray data were deposited in the Gene Expression Omnibus database under the GEO Series Accession No. GSE69465. We performed a microarray experiment for each sample without taking replicates. Total RNA was extracted from GIST-T1 parental and persister cells (GIST-T1 treated with 2 µM imatinib for 7 days) using the RNeasy Kit (Qiagen, Valencia, CA). RNA quality was assessed using the Agilent Model 2100 Bioanalyzer (Agilent Technologies, Palo Alto, CA). Two micrograms of total RNA were processed for microarray experiments using the Agilent Expression Array for One-Color (Agilent) according to the manufacturer's protocols. The resultant biotinylated cRNA was fragmented and hybridised to SurePrint G3 Human GE 8x60K v2 Microarray (Agilent). The arrays were washed, stained and scanned using the Gene Expression Hybridization Kit, Gene Expression Wash Buffers Pack and Agilent DNA Microarray Scanner (G2565CA), respectively. Expression values were generated using Feature Extraction software (Agilent). Each sample and hybridisation underwent quality-control evaluation.

Statistical analysis

Data have been presented as mean ± SD of the indicated values. To test for significant differences between two groups, the unpaired Student *t*-test was used. Two-sided *P*-values < 0.05 were considered significant. These analyses were carried out using JMP version 13.0 (SAS Institute, Cary, NC).

RESULTS

Characterisation of imatinib-derived GIST persister cells

In clinical practice, most patients with metastatic GIST achieve partial remission or stable disease after treatment with imatinib. However, we observed a small cluster of viable cells in the resected GIST specimen that was clinically well controlled with imatinib (Fig. 1a). We treated the GIST-T1 cell lines with imatinib after the plates reached 80–90% confluence. A small population of "quiescent" surviving persister cells were observed in the plates after treatment with imatinib for 9 days (Fig. 1b). Cell-cycle analysis revealed that the entire population of persister cells was in a G0–G1 cell fraction (Fig. 1c). Sensitivity to imatinib and cell proliferation were significantly decreased in persister cells ($P < 0.05$; Fig. 1d); however, these decreases were not observed in the cells which regrew 9 days after the cessation of imatinib (Fig. 1d, e).

Interestingly, sphere formation, a common characteristic of cancer stem cells, was not enhanced in the persister cells and was rather significantly deteriorated; $P < 0.05$; Supplemental Fig. 1A, B). Furthermore, the cells failed to show an increase in expression of mesenchymal markers (Supplemental Fig. 1C).

Metabolite analysis in GIST-T1 parental and imatinib-derived persister cells

As shown in the heatmap (Fig. 2a), the intracellular metabolites in cells that were incubated with imatinib were clearly different from the GIST-T1 parental cells. Moreover, glucose-related metabolism, including glycolysis and the pentose-phosphate pathway, was suppressed in persister cells, particularly in cells treated with imatinib for 14 days (Fig. 2b). Interestingly, glutathione metabolism was significantly suppressed in the persister cells compared with that in the parental cells.

Glutahione-related metabolism is suppressed in persister cells

As shown in Fig. 2c, the intracellular GSH level was significantly lower in persister cells than in parental cells ($P < 0.05$). Western blots revealed that the expression of GPX4, which plays a key role in regulating ferroptosis, was specifically reduced in persister cells (Fig. 2d). Further, we demonstrated that the levels of NADPH and glutathione reductase (GR) were significantly lower in persister cells than in parental cells ($P < 0.05$; Fig. 2e, f), which may result in reduced GSH levels in persister cells. Figure 2g shows a schematic outline of GSH metabolism.

Glucose metabolism is suppressed in persister cells

In accordance with the low level of NADPH, the glucose-uptake level was downregulated in persister cells ($P < 0.05$; Fig. 3a). The expression of glucose transporter (GLUT1), the dominant membrane transporter of glucose in cancer cells, was suppressed at the plasma membrane (Fig. 3b). Moreover, HIF-1α expression was downregulated in persister cells (Fig. 3c). Since glucose metabolism is involved in the metabolism of glutathione, we quantified GSH and NADPH in cells cultured in glucose-free medium for 9 days. Similar to persister cells, both GSH and NADPH were significantly reduced in cells cultured in glucose-free medium compared to the parental cells (Fig. 3d, e).

Vulnerability to ferroptotic cell death in persister cells

Chemosensitivity assay of RSL3, which is the most widely distributed GPX4 inhibitor, revealed significantly higher sensitivity for RSL3 in persister cells compared with the parental cells ($P < 0.05$; Fig. 4a). To test whether RSL3 induces ferroptotic cell death, we treated persister cells with a series of anti-ferroptotic compounds. Ferroptosis is known as iron-dependent cell death; therefore, we tested whether iron chelation rescued persister cells from cell death induced by GPX4 inhibition. Notably, 100 µM deferoxamine successfully rescued the persister cells from GPX4 inhibition (Fig. 4b). Moreover, we found that co-treatment with ferrostatin-1, which is a lipophilic antioxidant, rescued persister cells from cell death induced by GPX4 inhibition (Fig. 4c). Flow cytometric analysis revealed a remarkable increase in CellROX staining of reactive oxygen species, which implies that GPX4 inhibition induced lipid peroxidation only in persister cells (Fig. 4d). Furthermore, the reactive oxygen species activity level decreased back to normal on treatment with 100 µM deferoxamine (Fig. 4d,

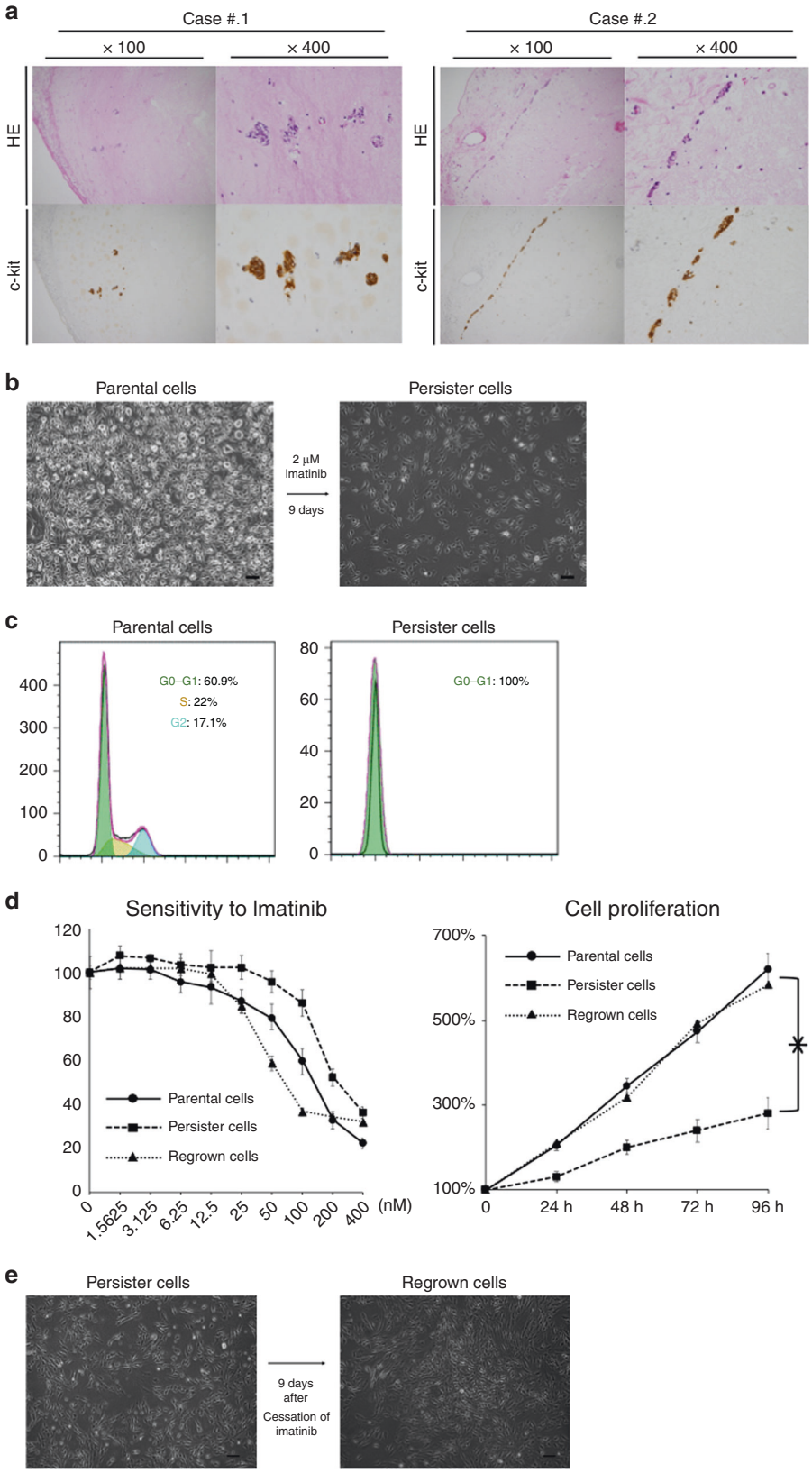

Fig. 1 Characterisation of imatinib-derived gastrointestinal stromal tumour (GIST) persister cells. a Immunohistoschemistry analysis on resected specimen of GIST, which is clinically well controlled with imatinib. A small cluster of viable cells can be seen. HE Hematoxylin Eosin. **b** A small fraction of GIST-T1 cells enter into a dormant drug-tolerant "persister" state in response to ≥9 days of 2 μM imatinib treatment (right). Scale bars, 200 μm. **c** Cell-cycle assay of GIST-T1 parental cells (left) and persister cells (right). **d** Chemosensitivity assay (left) and cell proliferation assay (right) of parental cells, persister cells and regrown cells. Scale bars, 200 μm. Chemosensitivity was indicated by viability after treatment with imatinib for 72 h. **e** Persister cells showed regrowth after 9 days of "drug-holiday" of imatinib. Data represent mean ± SD ($n = 6$), *$P < 0.05$.

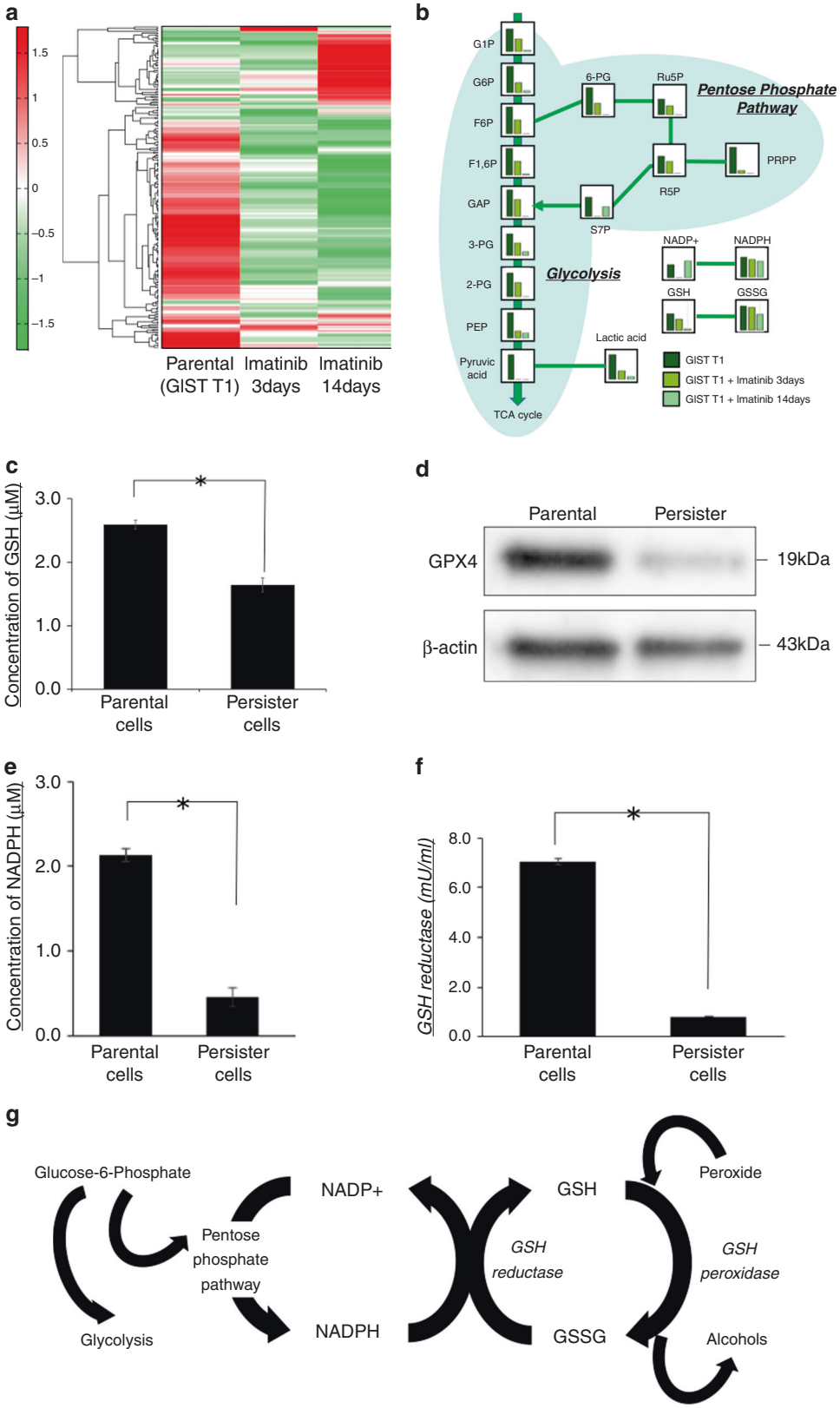

Fig. 2 GSH-related metabolic change in persister cells. a Heatmap analysis of metabolomes from gastrointestinal stromal tumour (GIST)-T1 parental cells and cells treated with imatinib for 3 and 14 days. **b** The detailed results of metabolome analysis, which focused on the glucose-related metabolites. **c** Intracellular concentration of glutathione (GSH) in parental and persister cells measured by GSH-Glo assay. Data represent mean ± standard deviation (SD) ($n = 4$), *$P < 0.05$. **d** Western blotting analysis of GPX4 in parental and persister cells. **e** Intracellular concentration of NADPH in parental and persister GIST-T1 cells was measured by NADP/NADPH assay. Data represent mean ± SD ($n = 4$), *$P < 0.05$. **f** Intracellular concentration of glutathione reductase of parental and persister cells measured by the OxiSelect Glutathione Reductase Assay Kit. Data represent mean ± SD ($n = 4$), *$P < 0.05$. **g** Schematic of a pathway that characterises the GSH-related metabolism.

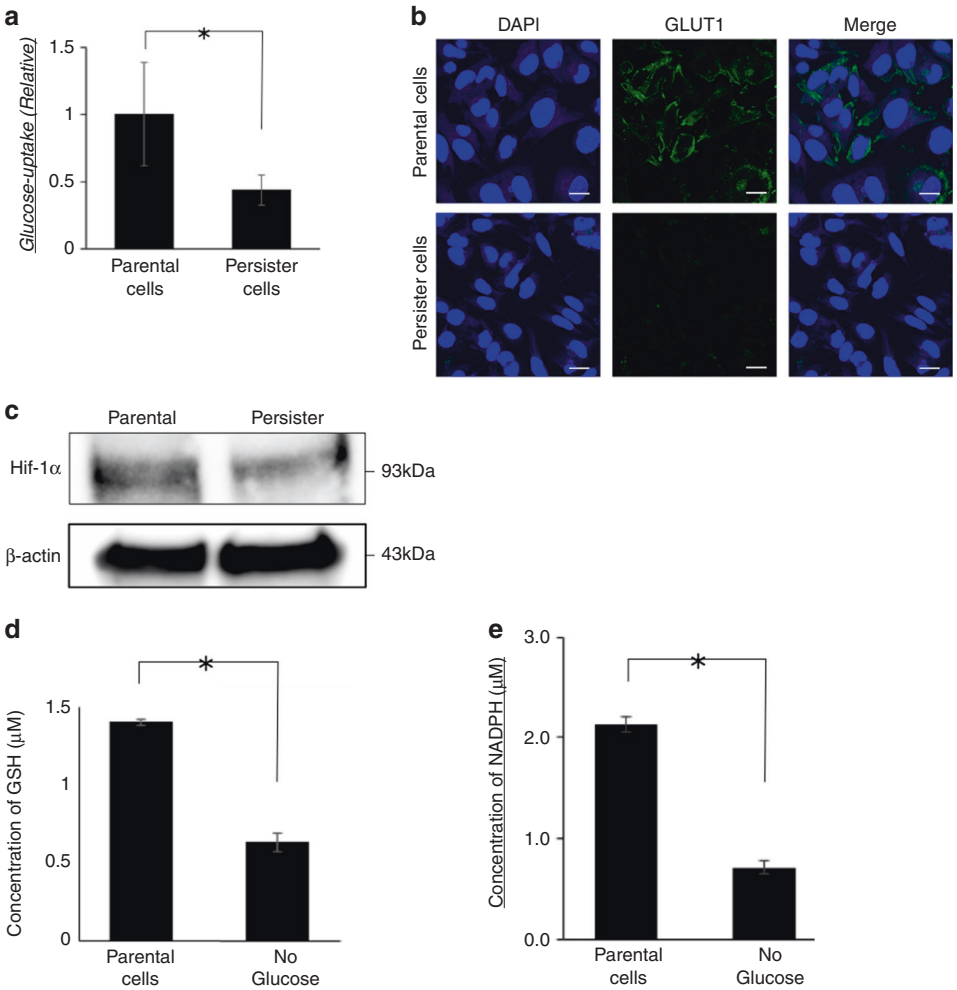

Fig. 3 Glucose-related metabolism was altered in persister cells. a The levels of glucose uptake in parental and persister gastrointestinal stromal tumour (GIST)-T1 cells. Data represent mean ± standard deviation (SD) ($n = 4$), *$P < 0.05$. **b** Immunofluorescence staining of glucose transporter 1 (GLUT1) using GIST-T1 parental cells or persister cells. Scale bars, 20 μm. **c** Western blotting analysis of Hypoxia-inducible factor (HIF)-1α in GIST-T1 parental cells of persister cells. **d** Intracellular concentration of glutathione (GSH) in parental cells and cells incubated in glucose-free medium for 9 days measured by GSH-Glo assay. Data represent mean ± SD ($n = 4$), *$P < 0.05$. **e** Intracellular concentration of NADPH in parental cells and cells incubated in glucose-free medium for 9 days was measured by NADP/NADPH assay. Data represent mean ± SD ($n = 4$), *$P < 0.05$.

green line). The apoptotic effects of RSL3 and its inhibition by deferoxamine and Z-VAD, a known caspase inhibitor, were evaluated by flow cytometry after staining with annexin V and PI (Fig. 4e). Particularly in persister cells, RSL3 increased the cell death fraction (top-right and bottom-right areas of each graph). Iron chelation with deferoxamine successfully rescued persister cells from RSL3-induced cell death. On the contrary, cell death induced by GPX4 inhibition in persister cells was not rescued by the pan-caspase inhibitor Z-VAD, which was consistent with the non-apoptotic nature of ferroptosis. In addition, we found that the addition of RSL3 to persister cells did not increase the caspase activity (Fig. 4f).

GPX4 inhibition suppressed tumour regrowth after imatinib therapy cessation in vivo

To confirm the antitumorigenic effect of GPX4 inhibition by RSL3, we used the tumour mouse model in which GIST-T1 cells were implanted subcutaneously. The subcutaneous tumour model mice were treated with RSL3 alone, imatinib alone, or the combination of RSL3 with imatinib (Fig. 5a). Compared with imatinib alone, the combination of RSL3 with imatinib remarkably suppressed tumour regrowth after imatinib cessation (Fig. 5b). RSL3 alone did not reduce tumour volume compared with the vehicle control. The immunohistochemical analysis of the tumour specimens on Day 21 showed no reduction of the number of c-kit (+) cells or Ki-67 (+) cells after RSL3 treatment, reflecting tumour regrowth after cessation of imatinib (Fig. 5c). The body weight gradually decreased in the imatinib-alone and combination groups during the imatinib administration period (days 1–9) and recovered to the baseline level several days after the cessation of imatinib (Fig. 5d). RSL3 did not affect the body weight in any group. We performed additional immunohistochemical analysis on mice treated with drugs in the same manner as in Fig. 5a (Fig. 5e), and revealed a reduction of viable cells in tumours from the combination group compared with that in the imatinib-alone group on day 12 (3 days after cessation of imatinib; Fig. 5f).

Validation in other cell lines

To further examine the anti-tumour effect of RSL3 in persister cells derived from other cell lines, we established gefitinib-derived or 5-FU-derived PC9 (non-small cell lung cancer cell line) persister cells similarly as the imatinib-derived GIST-T1 persister cells (Fig. 6a). The intracellular GSH level was significantly decreased in gefitinib-derived

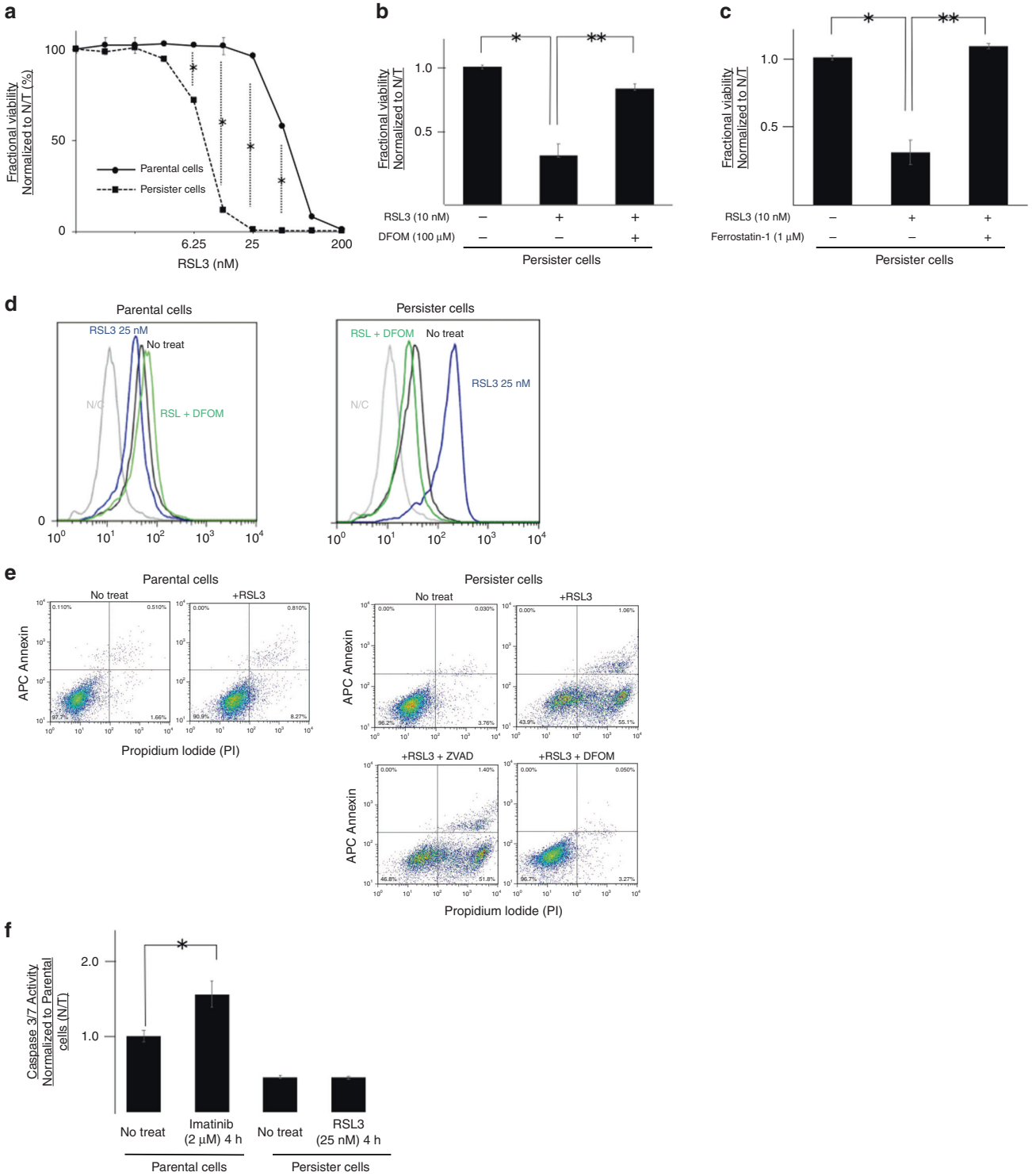

Fig. 4 Persister cells are vulnerable to glutathione peroxidase 4 (GPX4) inhibition. a Fractional viability of gastrointestinal stromal tumour (GIST-T1) parental cells and persister cells treated with indicated concentrations of RSL3 (GPX4 inhibitor). Cell viability was determined by Cell-titer Glo. **b, c** Fractional viability of GIST-T1 persister cells treated with RSL3 and co-treated with the iron-chelator deferoxamine (**b**) or the lipophilic antioxidant ferrostatin-1 (**c**). Cell viability was determined by Cell-titer Glo. Data represent mean ± standard deviation (SD) ($n = 6$), *$P < 0.05$. **d** Flow cytometry showing the expression of CellROX in parental cells or persister cells after 72 h treatment with RSL3 and deferoxamine. **e** Annexin V-APC/PI apoptosis assay carried out by BD FACS Canto™ II flow cytometry using Annexin V-APC and PI staining on GIST-T1 parental cells or persister cells treated with RSL ± DFOM or pan-caspase inhibitor Z-VAD. **f** Caspase activity after imatinib treatment for parental cells and RSL3 treatment for persister cells measured by Caspase 3/7-Glo Assay. Data represent mean ± SD ($n = 4$), *$P < 0.05$.

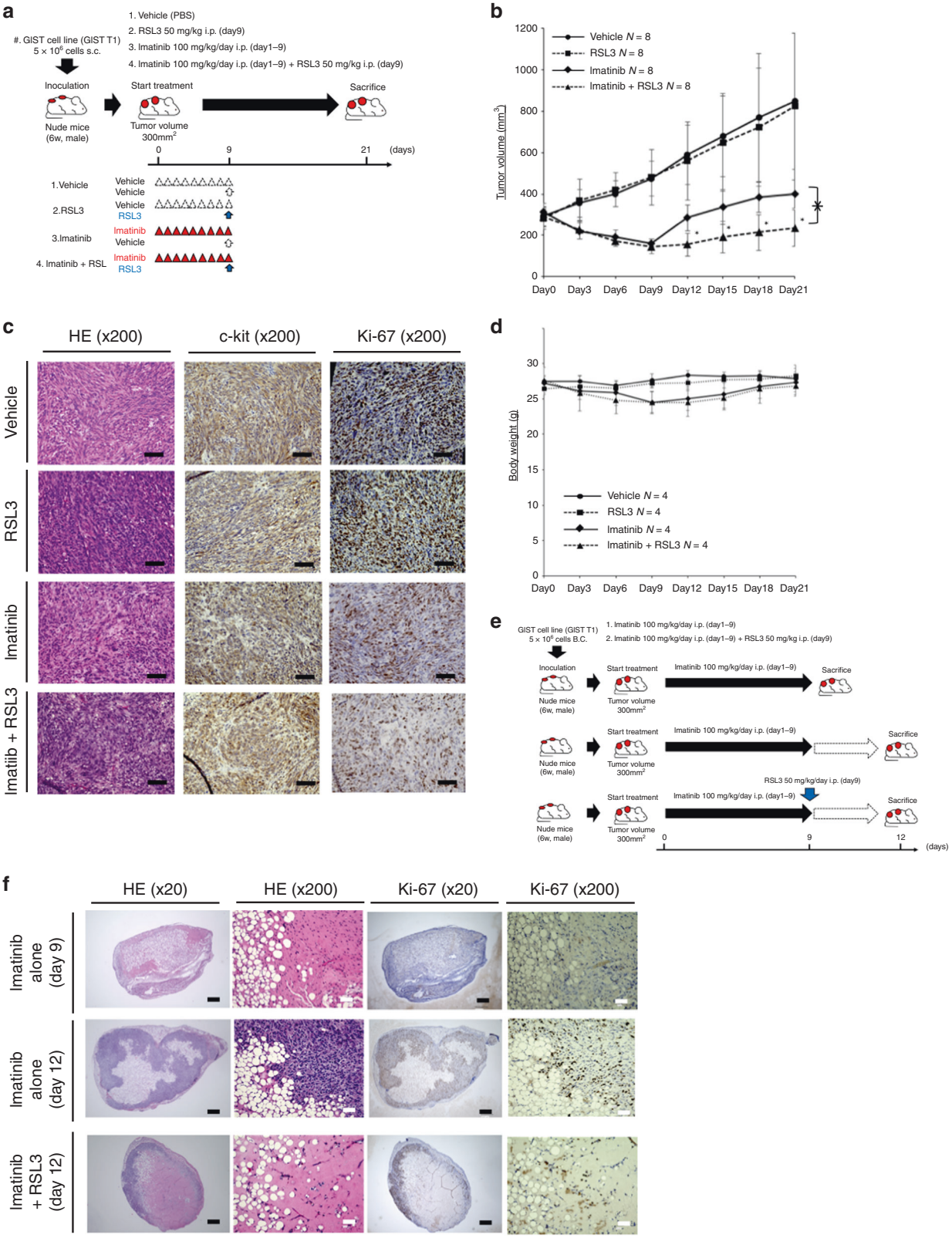

persister cells, but not significantly decreased in 5-FU-derived persister cells (Fig. 6b). Western blot analysis revealed a decrease in expression of GPX4 only in gefitinib-derived persister cells (Fig. 6c). A significantly higher sensitivity for RSL3, which was also observed in the imatinib-derived GIST-T1 persister cells, was observed only in gefitinib-derived persister cells (Fig. 6d). Moreover, we investigated the effect of RSL3 in an imatinib-resistant cell line, GIST-R8. The intracellular GSH level was significantly higher in GIST-R8 compared with that in GIST-T1 (Fig. 6e) and, thus, a significantly lower sensitivity for RSL3 was observed in GIST-R8 (Fig. 6f).

Fig. 5 Subcutaneous tumour model established to analyze the effect of RSL3. a 5.0×10^6 gastrointestinal stromal tumour (GIST)-T1 cells were transplanted subcutaneously into the dorsolateral aspect of male nude mice (6 weeks old). When the diameter of the subcutaneous tumours on either side reached 300 mm^3, each animal was treated with the vehicle ($n = 4$), RSL3 alone (on Day 9 at a dose of 50 mg/kg/day; $n = 4$) or imatinib alone (100 mg/kg once every day for 9 days; $n = 4$) or a combination of both (imatinib plus RSL3; $n = 4$). **b** To evaluate changes in tumour volume after each therapeutic regimen, the tumour volume was measured once every 3 days until 21 days from the initiation of therapy. Tumour volumes were determined by measuring the tumour length and width: volume = (width² × length)/2. Data represent mean ± standard deviation (SD) ($n = 8$), $^*P < 0.05$. **c** Hematoxylin and eosin, c-kit or Ki-67-stained sections of tumours from one representative mouse in each treatment group. Scale bars, 200 μm. **d** Body weight was measured every 3 days until Day 21. Data represent mean ± SD ($n = 4$), $^*P < 0.05$. **e** A subcutaneous tumour model was established in the same manner as shown in panel **a**. To analyze the effect of RSL3 on early phase, animals were sacrificed on day 9 or 12. **f** Hematoxylin and eosin, c-kit or Ki-67-stained sections of tumours from one representative mouse in imatinib-alone group on Day 9 (immediately after the withdrawal of imatinib), on Day 12 (3 days after the withdrawal of imatinib) or in the combination group on Day 12 (3 days after the withdrawal of imatinib). Scale bars, Black 500 μm. White 50 μm.

Glutathione (GSH) concentration and GPX4 expression in clinical samples

In the five clinical tumour samples resected after imatinib administration, the amount of GSH present in 100 mg of tumour was significantly lower than in the five clinical tumour samples resected without imatinib at the same time (Supplemental Fig. 2A, B).

A comparison of GPX4 expression in tissues before and after imatinib treatment in three patients whose biopsy specimens contained GIST cells among the resected patients after imatinib treatment showed that the expression of GPX4 in residual cells after imatinib treatment was lower than that in cells before imatinib treatment (Supplemental Fig. 2C).

DISCUSSION

In recent years, there has been increasing evidence of the existence of small populations of cancer cells that have evaded strong drug stress by entering a dormant state with negligible growth [19–21]. These populations of dormant cells are called "persister cells" [21]. It has been hypothesised that this drug-tolerant dormant state may contribute to the acquisition of bona fide, genetically driven, resistance mechanisms through long-term dormancy [21–23]. We have previously reported the establishment of imatinib-resistant GIST cells with additional kinase domain mutations by continuously culturing cells in imatinib for more than 6 months [17]. We focused on the resistance development process and postulated that the mutant resistant cells evoked from the small population of dormant cells could have survived long-term imatinib stress. Furthermore, we investigated these dormant "persister" cells by using DNA microarray analysis on differentially expressed genes and detected the depletion of expression of genes related to cell-cycle transition [17]. Therefore, as we explored the epigenetic character, we first evaluated the differences in the metabolism in the present study. The metabolite analysis revealed that intracellular metabolites in persister cells were completely different from the GIST-T1 parental cells or imatinib-resistant cells (Fig. 2a, b). Therefore, we hypothesised that the drug-tolerant persister GIST cells might provide a latent reservoir of cells for mutational drug resistance after they enter a dormant state with an altered metabolism. In addition, the characteristics of persister cells disappeared and they were restored to their original condition immediately after the removal of imatinib treatment (Fig. 1d). However the mechanism that triggers this change remains unknown. There are some clinical data which imply that persister cells are relevant to tumour regrowth and recurrence in clinical practice for GIST. We have confirmed that a very small population of viable cells often survive in hyarinized tissue in resected tumour specimens, which were clinically well controlled by imatinib (Fig. 1a). This very small population of persister cells may get reactivated after the discontinuation of imatinib, and could consequently contribute to recurrence, as described in the BFR14 trial [24]. To the best of our knowledge, this is the first study to have targeted imatinib-derived persister GIST cells for as a novel strategy for reducing drug resistance, tumour recurrence and metastasis.

The detailed mechanism that supports the survival of persister cells in drug stress is unclear. In this study, we demonstrated that the cell cycle of persister cells was arrested in G0/G1 (Fig. 1c). This G0/G1 arrest may provide tolerance to drug stress and may block cell proliferation, as shown in Fig. 1d. However, these characteristics were proved to be transient and of a reversible nature as the cell proliferation activity and sensitivity to imatinib recovered to the same levels as that of parental cells after 7 days of imatinib withdrawal (Fig. 1d). Furthermore, the sphere-formation activity of persister cells was not higher than that of parental cells (Supplemental Fig. 1B), which implies that persister cells may have different characteristics from that of cancer stem cells. In addition, microarray expression analysis revealed that RNA expression epithelial-mesenchymal transition markers did not vary between parental and persister cells (Supplemental Fig. 1C). Considering these facts, persister cells have a unique system to survive in imatinib stress which is distinct from cancer stems cells; however, the exact mechanism of survival is unclear.

Ferroptosis is a new form of regulated but non-apoptotic cell death that is caused by overwhelming iron-dependent lipid peroxidation [10, 11]. GPX4 is the primary enzyme that prevents ferroptosis by converting lipid hydroperoxides into non-toxic lipid alcohols [14, 25]; thus, GPX4 inhibitors are inducers of ferroptosis. GSH, a tripeptide and one of the most abundant free radical scavengers in the cell, is also known to be one of the most potent regulators of ferroptosis [26]. Hangauer et al. reported that drug-tolerant persister cells deplete of GSH showed high sensitivity to ferroptosis that was induced by GPX4 inhibitors in several cancer cell lines, including breast, ovarian and lung cancers and malignant melanoma [15]. Notably, we could validate the efficacy of GPX4 inhibitors in GSH-depleted gefitinib-derived persister PC9 cells, but not in GSH-maintained cell lines, including 5-FU-derived persister cells and GIST-R8 cells (Fig. 6). Therefore, GSH may be a very essential factor to evade ferroptotic death that is induced by GPX4 inhibition. Similarly, the expression of GPX4 (*Glutathione* peroxidase 4) was downregulated in the cells where GSH level was low. We speculated that GPX4 is an enzyme that is essential for survival and the cells can survive the oxidative stress if a small amount of its activity remained. Since both GPX4 expression and activity are lower in persister cells, the for the generation of ferroptosis by the GPX4 inhibition might be lower. In agreement with the disability to defend themselves from lipid peroxidation due to GSH depletion, we observed a marked increase in CellROX staining of reactive oxygen species after GPX4 inhibition by RSL3 only in persister cells (Fig. 4d). We further confirmed that co-treatment with a lipophilic antioxidant efficiently rescued persister cells from cell death that was induced by GPX4 inhibition (Fig. 4c). In addition, we observed that deferoxamine partially rescued persister cells, which implies that iron is an essential agent for cell death induced by GPX4 inhibition (Fig. 4b). However, consistent with the non-apoptotic nature of ferroptosis, the Z-VAD did not rescue persister cells from cell injury induced by GPX4 inhibition

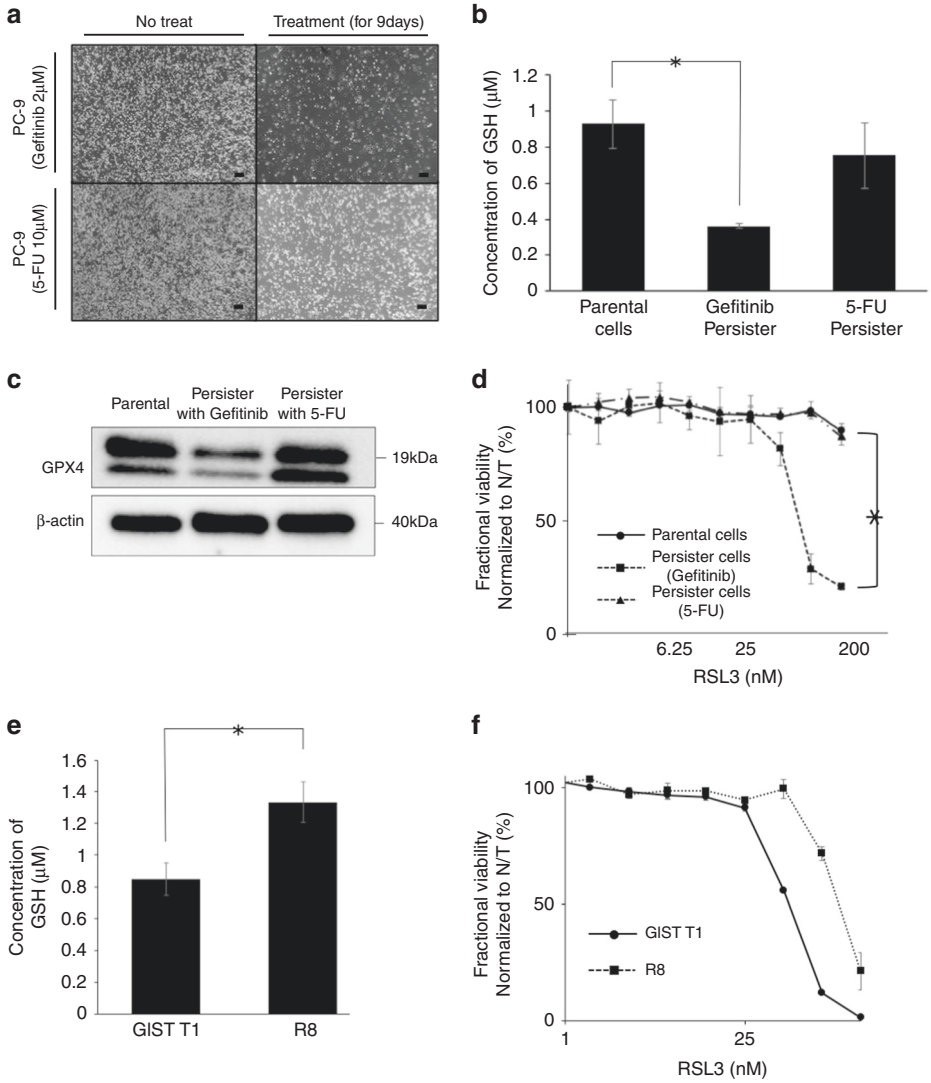

Fig. 6 The characteristics of persister cells and the effect of RSL3 (glutathion peroxidase 4 [GPX4] inhibitor) on persister cells in other cell lines (epidermal growth factor receptor (EGFR)-mutant lung cancer cell line PC9 and mutational imatinib-resistant gastrointestinal stromal tumour [GIST] cell line GIST-R8). a A small fraction of PC9 cells survived through ≥9 days of treatment with 2 μM gefitinib or 10 μM 5-fluorouracil (FU). Scale bars, 200 μm. **b** Intracellular concentration of glutathione (GSH) in PC9 parental and gefitinib-derived persister or 5-FU-derived persister cells measured by GSH-Glo assay. Data represent mean ± standard deviation (SD) ($n = 4$), *$P < 0.05$. **c** Western blotting analysis of GPX4 in parental and gefitinib-derived persister or 5-FU-derived persister cells. **d** Fractional viability of PC9 parental cells, gefitinib-derived persister cells and 5-FU-derived persister cells treated with the indicated concentrations of RSL3. Cell viability was determined by Cell-titer Glo. Data represent mean ± SD ($n = 6$), *$P < 0.05$. **e** Intracellular concentration of GSH in GIST-T1 parental cells and the mutational imatinib-resistant GIST cell line, GIST-R8 measured by GSH-Glo assay (Promega). Data represent mean ± SD ($n = 4$), *$P < 0.05$. **f** Fractional viability of GIST-T1 parental cells and GIST-R8 cells treated with indicated concentrations of RSL3. Cell viability was determined by Cell-titer Glo Assay. Data represent mean ± SD ($n = 6$), *$P < 0.05$.

(Fig. 4e). Furthermore, It was found that caspase activity was not increased when RSL3 was administered to persister cells (Fig. 4f). In summary, cell death induced by GPX4 inhibition is an "iron-dependent" and "caspase-independent" type of cell death and may be caused by ferroptosis.

In any case, it is likely that GSH depletion contributes to the vulnerability to ferroptosis in persister cells. In GSH-related metabolism, NADPH plays a key role in maintaining intracellular GSH level by supporting the activity of GR, which catalyzes the reduction of glutathione disulfide (GSSG) to the sulfhydryl form GSH (Fig. 2G) [27]. Both NADPH and GR are known as reducing cofactors that have the ability to maintain GSH levels, and therefore they protect the cells from lipid peroxidation and prevent ferroptosis [28]. Our data revealed that these reducing cofactors were markedly reduced in persister cells (Fig. 2e, f), which may disturb the GSH–GSSG balance and ultimately provoke vulnerability to ferroptosis. Furthermore, the major source of NADPH is the pentose-phosphate pathway [28]. Based on our metabolomic analysis on persister cells, that revealed reduction in the levels of glucose-related metabolites (Fig. 2b), we hypothesised that the glucose-uptake process may be disabled in these cells. Notably, we found that glucose uptake was significantly downregulated in the persister cells (Fig. 3a). In general, cancer cells reprogram their metabolism to promote growth and proliferation [29, 30]. The prime example of this metabolic reprogramming is the promotion of glycolysis by increasing the rate of glucose uptake. This phenomenon, one of the hallmarks of cancer, is observed even in the presence of oxygen and in completely functional mitochondria, and is known as the Warburg effect, [29, 31]. Previous studies reported that HIF-1α plays a vital

role in the Warburg effect by mediating this metabolic alteration through the overexpression of GLUT, which increase glucose uptake into tumour cells [32, 33]. In this study, GLUT1 and HIF-1α expression was suppressed in persister cells (Fig. 3b, c). The decisive factor, which integrates the altered metabolism in persister cells, has not been identified, although altered glucose metabolism may be one of the pivotal events that contributes to the unique nature of persister cells. Previous studies have shown that activation of the phosphatidyl inositol-4,5-bisphosphate-3-kinase (PI3K)/Akt pathway can upregulate the HIF-1α protein translation [34, 35], regulate GLUT1 expression and thus enhance glucose uptake [36]. TKI, including imatinib and gefitinib, have been associated with inactivation of the Akt signaling pathway, which discourages cell growth, proliferation and survival. We can infer that the dramatical alteration of metabolic property may be due to these interactions of the downstream effects of TKI. As described in Fig. 6, GSH depletion and the subsequent vulnerability to GPX4 inhibitor were confined to TKI-derived persister cells, which supports this hypothesis. Further investigation is needed to identify the key factor, which integrates the metabolic alteration and gives persister cells their unique characteristic.

In vivo analysis on subcutaneous tumour models has demonstrated that GPX4 inhibitors had significant anti-tumour effects only against tumours after imatinib treatment for 9 days (Fig. 5), and this was consistent with the results of an in vitro analysis. The histological analysis on the tumours on day 21 (12 days after the cessation of imatinib) revealed no significant differences in the number of viable cells or mitotic count (Fig. 5c) due to the substantial regrowth of cells. To estimate the small differences in regrowth, we additionally investigated the tumours on day 12 (3 days after the cessation of imatinib) and found that GPX4 inhibitor could suppress cell mitosis and regrowth (Fig. 5e, f). Since there is no way to detect the development of ferroptosis histologically, we have not been able to prove that cell death induced by RSL3 treatment is ferroptosis in a vivo experimental system. Despite the limitation of the small sample size of this in vivo analysis, RSL3 may have a certain efficacy and safety in the mice models. Further investigation is warranted to optimised the dosage and administration schedule for the drug.

There are several limitations to this study. First, we examined only a single GIST cell line, because imatinib-sensitive GIST cell lines other than GIST-T1 are very rare and unavailable in Japan. However, we confirmed the similar results using the EGFR-mutated lung cancer cells, PC9. Although the imatinib-resistant GIST cell line with secondary mutations were also investigated in this study, further validation using other imatinib-naïve GIST cell lines could be carried out in a future study. Second, there are few clinical data to verify whether the in vitro persister cell models accurately reflect the clinical setting. We have demonstrated that GSH concentration and GPX4 expression in resected specimens of patients who underwent neoadjuvant imatinib therapy were significantly lower than that of patients treated with surgery alone (Supplemental Fig. 2). However, it was difficult to perform further evaluation because the number of viable cells was so small after imatinib administration. A single-cell analysis should be performed on the clinical samples to overcome this limitation; however, this has not been available so far. Finally, the trigger for the transformation into a "persister cell" has remained obscure. Gupta A et al. previously reported that a significant proportion of GIST cells were able to survive under imatinib therapy, entering in a state of reversible quiescence and activating an autophagy dependent survival mechanism [37]. In our microarray analysis, LC3A expression level was also upregulated and autophagy might be involved in the persistent state. Further investigation is necessary to detect the decisive factor, which integrates the unique nature of persister cells.

In conclusion, this study shows that a GPX4 inhibitor effectively inhibited the proliferation of imatinib-derived persister cells and was effective against gefitinib-derived EGFR-mutated lung cancer cells. These anti-tumour effects appear to be associated with the alteration of metabolism, including GSH depletion, which is a unique feature of TKI-derived persister cells. Accordingly, we propose that GPX4 inhibitors may be a promising drug therapy when combined with TKI to overcome the current problems of drug resistance in patients with GIST.

DATA AVAILABILITY

The datasets generated/analyzed during the current study are not publicly available as they contain private information pertaining to the research participants but are available on request from the corresponding author (TT).

REFERENCES

1. Hirota S, Isozaki K, Moriyama Y, Hashimoto K, Nishida T, Ishiguro S, et al. Gain-of-function mutations of c-kit in human gastrointestinal stromal tumors. Science. 1998;279:577–80.
2. Heinrich MC, Corless CL, Duensing A, McGreevey L, Chen CJ, Joseph N, et al. PDGFRA activating mutations in gastrointestinal stromal tumors. Science. 2003;299:708–10.
3. Demetri GD, von Mehren M, Blanke CD, Van den Abbeele AD, Eisenberg B, Roberts PJ, et al. Efficacy and safety of imatinib mesylate in advanced gastrointestinal stromal tumors. N Engl J Med. 2002;347:472–80.
4. Blanke CD, Demetri GD, von Mehren M, Heinrich MC, Eisenberg B, Fletcher JA, et al. Long-term results from a randomized phase II trial of standard- versus higher-dose imatinib mesylate for patients with unresectable or metastatic gastrointestinal stromal tumors expressing KIT. J Clin Oncol. 2008;26:620–5.
5. Demetri GD, Benjamin RS, Blanke CD, Blay JY, Casali P, Choi H, et al. NCCN Task Force report: management of patients with gastrointestinal stromal tumor (GIST)-update of the NCCN clinical practice guidelines. J Natl Compr Cancer Netw. 2007;5:S1–29.
6. Gramza AW, Corless CL, Heinrich MC. Resistance to tyrosine kinase inhibitors in gastrointestinal stromal tumors. Clin Cancer Res. 2009;15:7510–8.
7. Heinrich MC, Corless CL, Demetri GD, Blanke CD, von Mehren M, Joensuu H, et al. Kinase mutations and imatinib response in patients with metastatic gastrointestinal stromal tumor. J Clin Oncol. 2003;21:4342–9.
8. Debiec-Rychter M, Dumez H, Judson I, Wasag B, Verweij J, Brown M, et al. Use of c-KIT/PDGFRA mutational analysis to predict the clinical response to imatinib in patients with advanced gastrointestinal stromal tumours entered on phase I and II studies of the EORTC Soft Tissue and Bone Sarcoma Group. Eur J Cancer. 2004;40:689–95.
9. Ramirez M, Rajaram S, Steininger RJ, Osipchuk D, Roth MA, Morinishi LS, et al. Diverse drug-resistance mechanisms can emerge from drug-tolerant cancer persister cells. Nat Commun. 2016;7:10690.
10. Stockwell BR, Friedmann AJP, Bayir H, Bush AI, Conrad M, Dixon SJ, et al. Ferroptosis: a regulated cell death nexus linking metabolism, redox biology, and disease. Cell. 2017;171:273–85.
11. Dixon SJ, Lemberg KM, Lamprecht MR, Skouta R, Zaitsev EM, Gleason CE, et al. Ferroptosis: an iron-dependent form of nonapoptotic cell death. Cell. 2012;149:1060–72.
12. Conrad M, Angeli JP, Vandenabeele P, Stockwell BR. Regulated necrosis: disease relevance and therapeutic opportunities. Nat Rev Drug Discov. 2016;15:348–66.
13. Yang WS, Stockwell BR. Ferroptosis: death by lipid peroxidation. Trends Cell Biol. 2016;26:165–76.
14. Yang WS, SriRamaratnam R, Welsch ME, Shimada K, Skouta R, Viswanathan VS, et al. Regulation of ferroptotic cancer cell death by GPX4. Cell. 2014;156:317–31.
15. Hangauer MJ, Viswanathan VS, Ryan MJ, Bole D, Eaton JK, Matov A, et al. Drug-tolerant persister cancer cells are vulnerable to GPX4 inhibition. Nature. 2017;551:247–50.
16. Saito Y, Takahashi T, Obata Y, Nishida T, Ohkubo S, Nakagawa F, et al. TAS-116 inhibits oncogenic KIT signalling on the Golgi in both imatinib-naïve and imatinib-resistant gastrointestinal stromal tumours. Br J Cancer. 2020;122:658–67.
17. Takahashi T, Elzawahry A, Mimaki S, Furukawa E, Nakatsuka R, Nakamura H, et al. Genomic and transcriptomic analysis of imatinib resistance in gastrointestinal stromal tumors. Genes Chromosomes Cancer. 2017;56:303–13.
18. Sugase T, Takahashi T, Serada S, Fujimoto M, Hiramatsu K, Ohkawara T, et al. SOCS1 gene therapy improves radiosensitivity and enhances irradiation-induced DNA damage in esophageal squamous cell carcinoma. Cancer Res. 2017;77:6975–86.
19. Dawson CC, Intapa C, Jabra-Rizk MA. "Persisters": survival at the cellular level. PLoS Pathog. 2011;7:e1002121.
20. Lantermann AB, Chen D, McCutcheon K, Hoffman G, Frias E, Ruddy D, et al. Inhibition of casein kinase 1 alpha prevents acquired drug resistance to erlotinib in EGFR-mutant non-small cell lung cancer. Cancer Res. 2015;75:4937–48.

21. Sharma SV, Lee DY, Li B, Quinlan MP, Takahashi F, Maheswaran S, et al. A chromatin-mediated reversible drug-tolerant state in cancer cell subpopulations. Cell. 2010;141:69–80.
22. Oxnard GR. The cellular origins of drug resistance in cancer. Nat Med. 2016;22:232–4.
23. Hata AN, Niederst MJ, Archibald HL, Gomez-Caraballo M, Siddiqui FM, Mulvey HE, et al. Tumor cells can follow distinct evolutionary paths to become resistant to epidermal growth factor receptor inhibition. Nat Med. 2016;22:262–9.
24. Patrikidou A, Chabaud S, Ray-Coquard I, Bui BN, Adenis A, Rios M, et al. Influence of imatinib interruption and rechallenge on the residual disease in patients with advanced GIST: results of the BFR14 prospective French Sarcoma Group randomised, phase III trial. Ann Oncol. 2013;24:1087–93.
25. Ingold I, Berndt C, Schmitt S, Doll S, Poschmann G, Buday K, et al. Selenium utilization by GPX4 is required to prevent hydroperoxide-induced ferroptosis. Cell. 2018;172:409–22.e421.
26. Proneth B, Conrad M. Ferroptosis and necroinflammation, a yet poorly explored link. Cell Death Differ. 2019;26:14–24.
27. Patra KC, Hay N. The pentose phosphate pathway and cancer. Trends Biochem Sci. 2014;39:347–54.
28. Shimada K, Hayano M, Pagano NC, Stockwell BR. Cell-line selectivity improves the predictive power of pharmacogenomic analyses and helps identify NADPH as biomarker for ferroptosis sensitivity. Cell Chem Biol. 2016;23:225–35.
29. Bose S, Le A. Glucose metabolism in cancer. Adv Exp Med Biol. 2018;1063:3–12.
30. Luengo A, Gui DY, Vander Heiden MG. Targeting metabolism for cancer therapy. Cell Chem Biol. 2017;24:1161–80.
31. Warburg O. On the origin of cancer cells. Science. 1956;123:309–14.
32. Chen C, Pore N, Behrooz A, Ismail-Beigi F, Maity A. Regulation of glut1 mRNA by hypoxia-inducible factor-1. Interaction between H-ras and hypoxia. J Biol Chem. 2001;276:9519–25.
33. Denko NC. Hypoxia, HIF1 and glucose metabolism in the solid tumour. Nat Rev Cancer. 2008;8:705–13.
34. Jiang BH, Jiang G, Zheng JZ, Lu Z, Hunter T, Vogt PK, et al. Phosphatidylinositol 3-kinase signaling controls levels of hypoxia-inducible factor 1. Cell Growth Differ. 2001;12:363–9.
35. Semenza G. Signal transduction to hypoxia-inducible factor 1. Biochem Pharmacol. 2002;64:993–8.
36. DeBerardinis RJ, Lum JJ, Hatzivassiliou G, Thompson CB. The biology of cancer: metabolic reprogramming fuels cell growth and proliferation. Cell Metab. 2008;7:11–20.
37. Gupta A, Roy S, Lazar AJ, Wang WL, McAuliffe JC, Reynoso D, et al. Autophagy inhibition and antimalarials promote cell death in gastrointestinal stromal tumor (GIST). Proc Natl Acad Sci USA. 2010;107:14333–8.

ACKNOWLEDGEMENTS

We would like to thank Editage (www.editage.jp) for English language editing.

AUTHOR CONTRIBUTIONS

TI wrote the initial draft of the manuscript. TT contributed to the analysis and interpretation of data and assisted in the preparation of the manuscript. All coauthors contributed to data collection and interpretation, and critically reviewed the manuscript. All authors approved the final version of the manuscript and agree to be accountable for all aspects of the work in ensuring that questions related to accuracy or integrity of any part of the work are appropriately investigated and resolved. Conception and design: TI and TT. Methodology development: TI and TT. Data acquisition: TI, RT and TT. Data analysis and interpretation: TI, TT, TN, SH, SS, MF, TN, YK, TS, KY, KT, KY, TM, MY, KN, HE and YD. Manuscript writing, review and/or revision: TI, TT, HE and YD. Study supervision: TT.

FUNDING INFORMATION

This work was not supported by any organizations besides Osaka University.

ETHICS APPROVAL AND CONSENT TO PARTICIPATE

The Human Ethics Review Committee of Osaka University Graduate School of Medicine approved the protocol for this retrospective study, and each participant provided written informed consent for study participation (ethical approval number: 27-061-002). All procedures were conducted in accordance with the principles underlying the Declaration of Helsinki and its later amendments.

CONSENT FOR PUBLICATION

Consent for publication has been obtained from the person whose data were on the paper.

COMPETING INTERESTS

The authors declare no competing interests.

ADDITIONAL INFORMATION

Supplementary information The online version contains supplementary material available at https://doi.org/10.1038/s41416-021-01566-9.

Correspondence and requests for materials should be addressed to Tsuyoshi Takahashi.

Reprints and permission information is available at http://www.nature.com/reprints

Publisher's note Springer Nature remains neutral with regard to jurisdictional claims in published maps and institutional affiliations.